Interpretation of Raman spectra of Ge/Si ultrathin superlattices

M. W. C. Dharma-wardana, G. C. Aers, D. J. Lockwood, and J.-M. Baribeau
Division of Physics, National Research Council of Canada, Ottawa, Canada K1A 0R6
(Received 13 June 1989)

We present a study of Raman scattering by phonons in Ge_mSi_n-type ultrathin superlattices. We calculate the Raman spectra of ideal unstrained structures and then successively include strain and interface smudging. The calculations reveal interesting systematics about quasiconfinement. It is shown that quasiconfinement, strain, and interface smudging have to be treated concurrently in the interpretation of observed spectra. The nature of the "Ge-Si"-like mode often seen in experimental spectra is elucidated. Using the information base built up from the study of theoretical spectra, we analyze experimental spectra of superlattices grown on Si(100) and Ge(100) substrates to obtain quantitative information useful for structural characterization of the samples studied.

I. INTRODUCTION

Ultrathin "atomic-layer" superlattices made up of pure Si and pure Ge atomic layers have been recently fabricated with the use of molecular-beam-epitaxy (MBE) techniques.[1] A versatile method for investigating the structural properties of these $(Ge_mSi_n)_p$ superlattices, where p is the number of repeats, is Raman spectroscopy. If the structures are grown on a Si substrate m is not more than six atomic layers, and p is such that the whole structure itself has a critical length. Thus we are dealing with a few hundred atomic layers grown on a Si substrate (say), and typically capped with 50 Å of a protective layer of silicon. In previous papers[2,3] we have studied the low-lying acoustic phonons ($\Delta\omega < 100$ cm^{-1}) in such structures and found them to be sensitive to the overall periodicities, boundary conditions, and average properties of the lattices. On the other hand, optical phonons are expected to yield information regarding local structure, interface smudging, and lattice-strain effects. The object of this paper is to interpret in detail the observed Raman spectra of $(Ge_mSi_n)_p$-type superlattices on the basis of an analysis of theoretical spectra of these systems. For this purpose we will calculate the Raman spectra of ideal unstrained $(Ge_mSi_n)_p$ structures, then successively include strain and interface smudging in the theoretical model. Since we are concerned with backscatteringlike Raman spectra for longitudinal vibrations along the [001] direction, we will use a linear-chain model[3] to calculate the phonons while a bond-polarizability approach[4,5] will be used to evaluate the Raman scattering intensity.

In Sec. II we discuss the details of the linear-chain model and the calculation of the Raman intensities. In Sec. III we present the results of the calculation for the ideal structures and bring out some interesting systematics. In Sec. IV we consider the effect of strain on the position of the principal Raman peaks for superlattices grown on Si or Ge substrates. The effect of strain is in many cases similar to the effect of interface smudging and this is considered in Sec. V. The results of Secs. III–V show that confinement, strain, and interface smudging need to be considered *together* in interpreting an experimental spectrum. In Sec. VI we use the information of the preceding sections as well as specific calculations and results of annealing studies to obtain an interpretation of the experimentally observed spectra of MBE-grown samples.

II. CALCULATION OF PHONONS AND RAMAN INTENSITIES

In our previous studies[2,3] we used a linear-chain model of the total structure

$$(\text{Si substrate})+(Ge_mSi_n)_p+(\text{Si cap}),$$

where the substrate was modeled by 1000 atomic layers of Si, while the Si cap of 50 Å was modeled by 37 atomic layers of Si. The first atomic layer of the substrate was assumed to be fully anchored while the surface layer (last layer of cap) was treated as free or anchored, depending on a parameter σ which specified the degree of anchoring. The $(Ge_mSi_n)_p$ superlattice itself was modeled in each case as m atomic layers of Ge and n atomic layers of Si, repeated p times. In our previous studies, only the low-frequency Raman spectra ($\Delta\omega < 100$ cm^{-1}) were considered. Hence a single nearest-neighbor force constant chosen to reproduce the Brillouin frequency was used. In this paper we propose to study the higher-frequency phonons covering a much larger range ($\Delta\omega > 90$ cm^{-1}) and hence a single-force-constant model becomes inadequate. On the other hand, these higher-frequency phonons are less sensitive to the sample-specific details like the presence or absence of a cap, surface boundary conditions, and the presence of a substrate. Nevertheless we have retained the sample-specific details in our modeling. Theoretical force constants k_1 to k_4 for bulk silicon[6] and germanium[7] up to fourth-neighbor interactions were used in the linear-chain model. For interactions between Si *and* Ge the arithmetic mean of the bulk force constants was used. Table I gives the values of the force constants as well as the multiplicative factor f (applied to each bulk force constant). This factor was necessary to reduce the calculated bulk Raman frequency of Si and Ge from 309.8 and 526.3 cm^{-1} to the values of

TABLE I. Parameters used for Ge_mSi_n superlattice calculations. The bulk force constants (Refs. 6 and 7) for Ge and Si, k_1 to k_4 up to fourth-neighbor interactions are given in units of 10^5 dyn/cm^2. A scale factor f is used to bring the calculated bulk Raman frequencies (309.8 and 526.3 cm^{-1}) for Ge and Si to the experimental values (300.6 and 520.1 cm^{-1}) at 298 K. The real and imaginary refractive indices η_1 and η_2 at 468 nm are given. The Raman tensor components (Ref. 11) relevant to backscattering along the z axis are α_{xx} and α_{xy}.

	Ge	Si
k_1	1.010	1.128
k_2	0.059	0.074
k_3	0.016	0.018
k_4	0.004	0.004
f	0.9426	0.9762
η_1	4.125	4.514
η_2	2.275	0.110
α_{xx}	9.93	3.32
α_{xy}	4.07	1.59

300.6 and 520.1 cm^{-1}, respectively, observed in our samples at 298 K. In our calculations we do not assume any translational invariance, etc., but simply diagonalize a matrix which is of dimensionality equal to $N_{\text{substrate}}+N_{\text{superlattice}}+N_{\text{cap}}$ where $N_{\text{substrate}}, N_{\text{superlattice}}$, and N_{cap} are the number of substrate, superlattice, and cap atomic layers, respectively. For the $\Delta\omega > 90$ cm^{-1} regime we used $N_{\text{substrate}}=500$ unless otherwise stated.

In our previous studies, for $\Delta\omega < 100$ cm^{-1}, the Raman intensities were calculated using a simple photoelastic coupling model. A more general model is needed for the present studies and we have adopted the bond-polarizability model[4,5] for calculating the Raman intensities. If the growth direction, i.e., the [001] direction, is designated the z axis, the backscattering along the z direction will lead to Raman signals with $z(xx)\bar{z}$ and $z(xy)\bar{z}$ polarizations.[8] The corresponding Raman intensities are proportional to the modulations $|\delta\chi^{xy}/\delta R_z|^2$ and $|\delta\chi^{xx}/\delta R_z|^2$, respectively, where R_z is the z component of the vector defining the bond and χ is the susceptibility tensor. The bond polarizability Π of Weber *et al.*[4] is proportional to χ and is written as

$$\Pi_{\alpha\beta}(\mathbf{R})=\frac{\mathbf{R}_\alpha\mathbf{R}_\beta}{R^2}\alpha_{\parallel}(R)+\left[\delta_{\alpha\beta}-\frac{\mathbf{R}_\alpha\mathbf{R}_\beta}{R^2}\right]\alpha_{\perp}(R) \quad (2.1)$$

where $\mathbf{R}$ is a vector along the bond and α and β designate x, y, and z components. The bond polarizabilities parallel ($\alpha_{\parallel}$) and perpendicular ($\alpha_{\perp}$) to the bond depend on the bond length R. When atomic planes parallel to the xy plane vibrate along the z axis, R_z changes and $\Pi_{\alpha\beta}$ is modulated. Menéndez *et al.*[9] have recently used this form of the bond-polarizability model to interpret a Raman study of a (Ge_4Si_4) superlattice. A strictly equivalent model introduced earlier by Bell[5] uses the mean polarizability P and the anisotropy γ to write

$$\Pi_{\alpha\beta}(\mathbf{R})=\left[P(\mathbf{R})\overleftrightarrow{\mathbf{I}}+\gamma(\mathbf{R})\left[\frac{\mathbf{RR}}{R^2}-\tfrac{1}{3}\overleftrightarrow{\mathbf{I}}\right]\right]_{\alpha\beta} \quad (2.2)$$

where $\overleftrightarrow{\mathbf{I}}$ is the unit tensor. Zhu and Chao[10] used this form of the bond-polarizability model in their studies on folded acoustic modes in superlattices. Only one-phonon Raman scattering is considered here. The bond distance $\mathbf{R}$, or more precisely $\mathbf{R}_{ij}$, connecting the ith atom with the jth-nearest bonded atom, can be expressed as $\mathbf{R}_{ij}=(\mathbf{r}_i+\mathbf{u}_i)-(\mathbf{r}_j+\mathbf{u}_j)$ where $\mathbf{r}_i,\mathbf{r}_j$ denote the positions of the unperturbed atoms while $\mathbf{u}_i,\mathbf{u}_j$ are the atomic displacements. Only terms linear in these displacements are retained in calculating the change in the susceptibility on changing R_z. Since we are interested in Raman scattering due to longitudinal vibrations along the z direction, reduction of (2.1) or (2.2) leads us to intensities I_{xx} and I_{xy} in the simple form

$$I_{xx}(\omega_j)\propto\left|\sum_{n=1}e^{iqz_{2n}}(a^{xx}_{2n-1}U^j_{2n-1}-a^{xx}_{2n+1}U^j_{2n+1})\right|^2,$$

$$I_{xy}(\omega_j)\propto\left|\sum_{n=1}e^{iqz_{2n}}(a^{xy}_{2n-1}U^j_{2n-1}+a^{xy}_{2n+1}U^j_{2n+1}-2a^{xy}_{2n}U^j_{2n})\right|^2, \quad (2.3)$$

where U_i^j is the displacement of the ith *atomic layer* along the [001] direction for the jth phonon mode. Note that the U_i occurring here refers to an average over the *atomic* displacements u_i taken over the atoms in the plane perpendicular to the linear chain. The phonon modes and displacements were calculated from the linear-chain model. In (2.3), the surface layer can be taken to be the first layer. The effect of the finiteness of the phonon wave vector q can be approximately included via the phase factor $\exp(iqz_{2n})$ which contains the position z_{2n} of the $2n$th atomic layer along the linear chain. Since the experimental optical modes of $(Ge_mSi_n)_p$-type structures tend to be broad the doublet splitting of folded modes introduced by the phase factor is negligible and can in general be ignored. However, we have retained this effect in our calculations and estimated q using the average refractive index of the material (see Table I). The polarizability constants a^{xx} and a^{xy} of each layer are proportional to α_{xx} and α_{xy} of Table I. These, in turn, can be related to α_1, α_q, and $\alpha_{25'}$, of Cardona[11] in the case of bulk materials. We also note that for Ge_mSi_n-type superlattices only the $z(xy)\bar{z}$ polarization produces a significant intensity. Hence the Raman intensities depend on the single parameter a^{xy} which may be thought of as an adjustable constant, deviating where necessary to some extent from the bulk values. For comparison with experimental spectra the calculated spectra were broadened (parameter Γ) to give a Lorentzian form such that

$$I(\omega)\propto\sum_j\frac{\Gamma/\pi}{(\omega-\omega_j)^2+\Gamma^2}[I_{xx}(\omega_j)+I_{xy}(\omega_j)]\frac{n(\omega_j)+1}{\omega_j}. \quad (2.4)$$

Here ω_j is the frequency of the jth mode and $n(\omega_j)$ is the usual Bose factor.

TABLE II. Calculated Raman peaks in ideal Ge_mSi_n structures. Only the four principal high-energy peaks ($\Delta\omega$ in cm^{-1}) are given. See also Fig. 1.

m/n	1	2	3	4	5	6	7	8
1	417	468, 192	489, 294	500, 359	506, 402	509, 431	512, 450	514, 464
				139	229	292, 109	338, 189	372, 247
2	409, 210	463, 253	487, 295	499, 352	505, 397	509, 427	512, 448	513, 462
			266	230	260	294, 201	338, 238	368, 265
3	402, 260	462, 275	486, 297	498, 349	505, 395	509, 426	512, 447	513, 462
		111	225	264	277	296, 241	332, 267	366, 278
4	401, 278	462, 285	486, 298	498, 348	505, 395	509, 426	512, 447	513, 462
	125, 108	176	251, 108	279, 155	286, 91	297, 260	331, 278	366, 286
6	401, 291	462, 293	486, 299	498, 348	505, 395	509, 426	512, 447	513, 462
	220, 88	237, 137	273, 202	291, 227	293, 243	298, 277	330, 291	366, 293

III. PHONONS AND RAMAN SPECTRA OF IDEAL Ge_mSi_n STRUCTURES

In this section we present results of calculations of Raman spectra for ideal Ge_mSi_n structures, i.e., structures with no strain or interface smudging. The calculation assumes a silicon substrate modeled by an adequate number of atomic layer (500 unless stated otherwise), p repetitions of Ge_mSi_n with p taken to be 24, followed by typically 37 atomic layers of Si to form a 50 Å cap. We study the prominent spectral features seen for frequency shifts $\Delta\omega$ greater than, say, 90 cm^{-1}.

Table II gives the four main calculated high-frequency features of the Raman spectra of $(Ge_mSi_n)_{24}$ structures. Figure 1 illustrates three typical spectra, obtained with a broadening Γ of 3 cm^{-1} at each peak.

The results of Table II show several interesting features. The Si-Si modes (which have $\Delta\omega > 300$ cm^{-1}) tend to be essentially independent of the Ge environment, as soon as $m > 1$ (see Fig. 2). This reflects the fact that the bulk Si optical vibrations form a band which does not overlap the Ge vibration bands and are hence essentially *confined*[12,13] to the Si slabs, with no penetration into the Ge layers. In Ge_mSi_n, we find that at $n=4$ there are two Si modes, viz., $\Delta\omega_1 \approx 498$ cm^{-1} and $\Delta\omega_2 \approx 349$ cm^{-1}. These correspond to the fully antisymmetric $\vec{Si}$-$\vec{Si}$-$\overleftarrow{Si}$-$\overleftarrow{Si}$ mode and the partially antisymmetric $\vec{Si}$-$\vec{Si}$-$\overleftarrow{Si}$-$\overleftarrow{Si}$ mode (see Fig. 3).

In going from, for example, $(Ge_2Si_6)_{24}$ to $(Ge_2Si_7)_{24}$ the Si-Si-like peaks at 509 and 427 cm^{-1} move upwards to 512 and 448 cm^{-1} due to the decrease in confinement. In addition, a new Si-Si-type mode appears at 338 cm^{-1}, while the Ge-Ge-like peak at 294 cm^{-1} drops down to 238 cm^{-1} (see Fig. 1). The next lowest significant peak in the calculated Raman spectrum of $(Ge_2Si_7)_{24}$ is at 104 cm^{-1} (In Table II we have only retained the four main high-energy peaks). Thus an additional Si vibrational mode appears near 335 cm^{-1} when n in Ge_mSi_n reaches 7. Once a new Si mode appears, at an appropriate value of n, its frequency is seen to be more or less independent of m in Ge_mSi_n.

Let us now consider the behavior of the Ge-Ge optical-mode vibrations. These vibrations are buried in the acoustic continuum of the Si vibrations and hence their behavior depends on the number n of the Si layers. If we follow the series Ge_2Si_n we see that the Ge-Ge vibration starts at 210 cm^{-1} for $n=1$ and reaches 295 cm^{-1} for $n=3$. This behavior recommences once again at 230 cm^{-1} for $n=4$ and reaches 294 cm^{-1} for $n=6$. The variation of the partially confined Ge-Ge optic-mode frequency as a function of the number of silicon layers shows a three-Si-atom cycle as shown in Fig. 2. This reflects the fact that three silicon atoms are approximately of the same mass as one Ge atom. Thus, for example, the Ge_2Si_9 system can approximate to a $Ge_2(\text{"Ge"})_3$ structure and hence the Ge-Ge optic mode approaches closer to the bulk value than, say, in a structure like Ge_2Si_{10}.

Figure 1 shows several Raman spectra calculated using the standard values of the bond polarizabilities (Table I). The two calculated spectra for Ge_2Si_4 correspond to free-

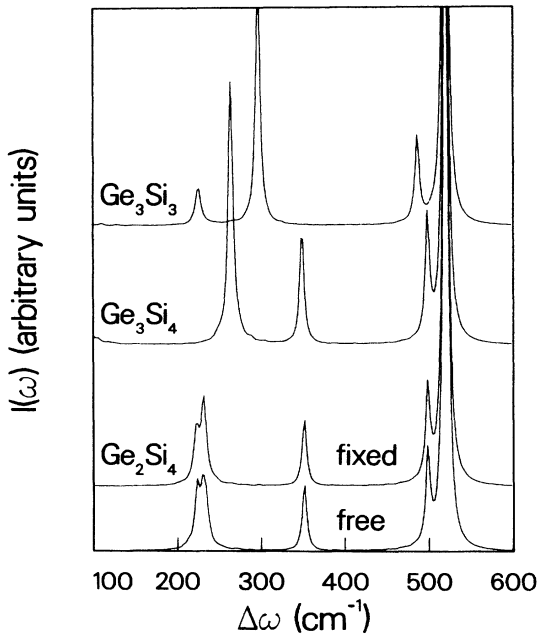

FIG. 1. Calculated Raman spectra of the structure (Si substrate)+$(Ge_mSi_n)_{24}$+(Si cap) for three typical cases. The intense peak at 520 cm^{-1} arises from substrate and cap Si layers. The peaks are broadened with $\Gamma=3$ cm^{-1}. The system $(Ge_2Si_4)_{24}$ has a low-frequency mode at 225 cm^{-1} which is somewhat sensitive to the surface boundary conditions.

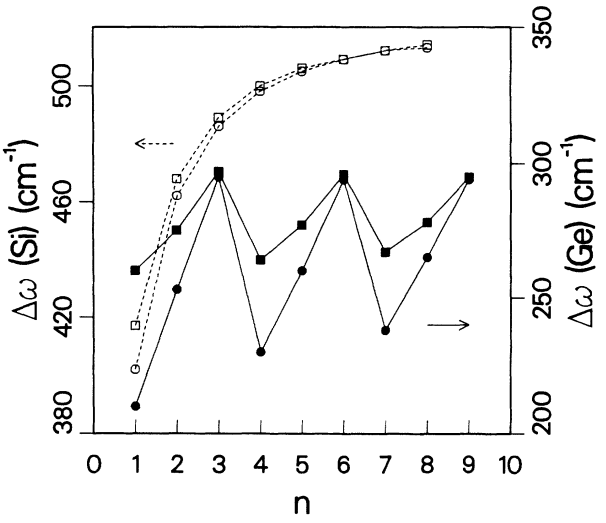

FIG. 2. Confined modes of Si and Ge. The open squares and circles show the highest Si-Si optical-phonon frequency in Ge_1Si_n and Ge_3Si_n respectively, as a function of Si-slab thickness n. The solid squares and circles show the highest Ge-Ge optical-phonon frequency in Ge_3Si_n and Ge_2Si_n respectively, as a function of n.

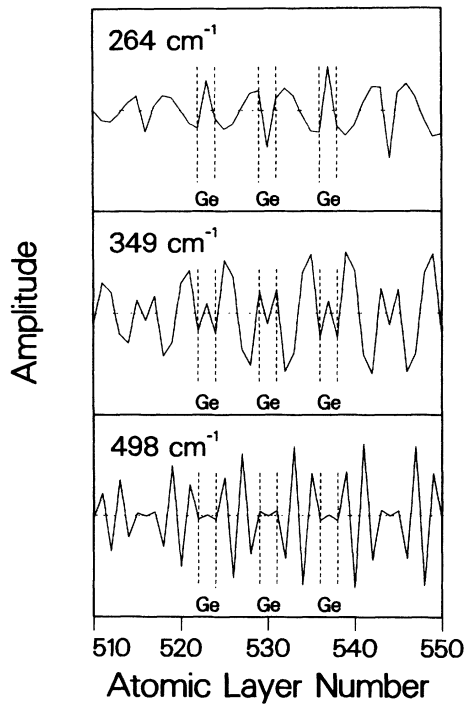

FIG. 3. Vibration amplitudes of the three peaks of (Si substrate)$+(Ge_3Si_4)_{24}+$(Si cap) shown in Fig. 1. The substrate has 500 atomic layers of Si. The partially antisymmetric Si-Si vibration at 349 cm^{-1} involves displacement of the Ge interface layers as well. Hence these modes have been called "Ge-Si" modes in the text. Only some of the Ge interface layers are shown as vertical dashed lines.

and fixed-surface-boundary conditions. Of the two peaks at $\Delta\omega=225$ and 230 cm^{-1} the lower one is somewhat sensitive to the surface boundary conditions used. This peak arises from a mode which develops a high amplitude near the surface region, while the peak at 230 cm^{-1} is the expected Ge-Ge vibration for the structure. Thus it is clear that even in studying optical phonons, sample-specific effects can sometimes be important.

IV. THE EFFECT OF STRAIN

Up to this point we have discussed ideal structures of the form (Si substrate)$+(Ge_mSi_n)_p+$(Si cap) using the force constants applicable to unstrained bulk silicon and germanium. However, if the substrate is silicon, pseudomorphic epitaxial growth requires that the in-plane lattice constant of the Ge layers match the smaller Si lattice constant. Hence the Ge layers are strained while the silicon layers are generally believed to be free of strain. In fact annealing studies which will be discussed later show that even the Si layers may have some strain in them. A complementary situation exists for growth on Ge substrates. By a comparison of the optical-phonon peaks observed from incommensurate Ge_xSi_{1-x} layers with those of commensurate alloy layers grown on silicon substrates, Cerdeira *et al.*[14] showed that strain can shift the so-called Ge-Ge, Ge-Si, and Si-Si optical vibration peaks to higher frequencies. Their studies suggest that the Ge-Ge vibrations, as well as the Ge-Si vibrations, could be shifted up by as much as 15 cm^{-1} for a fully strained system. The Si-Si peaks are even more sensitive to strain.

In a real superlattice of the form (Si substrate) $+(Ge_mSi_n)_p+$(Si cap) we have very little information regarding the microscopic strain profile [interface layers may be differently strained to those inside a Ge_m slab]. However, we will assume a simple model, to theoretically investigate the effect of strain on the Raman spectra. For $(Ge_mSi_n)_p$ structures grown on Si substrates we compare the spectra calculated using the four bulk force constants for Ge, and then with the bulk values increased by 10%, while keeping the Si force constants unchanged. Such a shift, $k_{Ge}\rightarrow 1.1k_{Ge}$, has the effect of moving the main Ge-Ge Raman peak by about 12 cm^{-1} and is of the desired magnitude as seen in experimental samples. We also do a series of calculations where the Si force constants are scaled *downwards* by 10%, i.e.. $k_{Si}\rightarrow 0.9k_{Si}$, while the Ge force constants are kept unchanged, as this simulates the behavior of (Ge substrate)$+(Si_nGe_m)_p$ $+$(Ge cap) structures where the Si slabs are strained.

In Table III we show in columns A the calculations for $(Ge_mSi_n)_p$ with strained Ge slabs, while columns B refer to strained Si slabs in $(Si_nGe_m)_p$. Since all structures of the form Ge_mSi_n with $m,n\leq 6$ have two Si-Si-like peaks ($\Delta\omega>300$ cm^{-1}) except in the case of Ge_mSi_2 we have chosen to call the highest peak ($\Delta\omega>400$ cm^{-1}) the Si-Si peak, while the lower peak has been called the Ge-Si peak. [For example, in Fig. 3 the vibration amplitudes for the Si-Si mode at 498 cm^{-1} and the "Ge-Si" mode at 349 cm^{-1} for Ge_3Si_4 are shown.] The reason for this nomenclature will become clearer by the time we discuss

TABLE III. Effect of strain on the main Raman peaks of $(Ge_mSi_n)_{24}$ superlattices. Structures on Si substrates are modeled by a 10% increase in the Ge force constants ($k_{Ge} \rightarrow 1.1k_{Ge}$) and the resulting upward (positive) shifts (cm^{-1}) are given in columns labeled A. Structures on Ge substrates are modeled by a decrease of Si force constants ($k_{Si} \rightarrow 0.9k_{Si}$) and the resulting downward (negative) shifts are given in B columns. The absolute positions can be obtained by adding the values to the unstrained peak positions given in Table II. The lower-frequency Si-Si peak is called the Ge-Si peak. (In the case of Ge_mSi_2 since there is only one Si-Si peak the same values are entered twice.) The effect of interface smudging and strain is also given for the $(Ge_6Si_6)_{24}$ structure (see text).

m,n	$\delta(\Delta\omega)$ Ge-Ge		$\delta(\Delta\omega)$ Ge-Si		$\delta(\Delta\omega)$ Si-Si	
	A	B	A	B	A	B
2, 2	8.7	−3.0	(4.0)	−(19)	(4.0)	−(19)
2, 4	8.2	−4.0	8.0	−12	1.4	−25
2, 6	6.4	−8.0	3.0	−19	0.5	−26
4, 2	13	−0.5	(4.4)	−(19)	(4.4)	−(19)
4, 4	11	−2.4	6.0	−12	1.5	−24
4, 6	10	−4.4	3.0	−19	0.5	−26
6, 2	14	0.0	(4.4)	−(19)	(4.4)	−(19)
6, 4	14	−0.5	6.0	−12	1.6	−24
6, 6	13	−2.0	3.0	−19	0.5	−26
Smudged 6, 6						
$x=0.15$	12	0.0	2.6	−40	0.3	−30
$x=0.30$	11	4.0	4.6	−53	0.9	−32

interface-smudging effects. In the case of Ge_mSi_2 only one Raman peak occurs for $\Delta\omega > 300$ cm^{-1}. The vibrations associated with this peak at about 462 cm^{-1} (see Table II) are not confined entirely to the Si slabs but also involve the Ge interface layers. Hence this mode cannot be classified either as a pure Si-Si mode or a Ge-Si mode and entries in Table III for Ge-Si and Si-Si peaks in Ge_2Si_2, Ge_4Si_2, and Ge_6Si_2 are thus put in parentheses and entered twice.

In Table III, column A for $\delta(\Delta\omega)$ (Ge-Ge) shows that the strain shift of the Ge-Ge peak depends both on m and n. Larger Ge slabs (larger m) show a bigger strain shift. The Ge-Si peak is less affected by an increase in k_{Ge} than the Ge-Ge peak. But significantly, the value of the strain shift depends on the silicon slab size n, going from 4 cm^{-1} to a maximum of 6–8 cm^{-1} and then down to 3 cm^{-1} for $n=6$. Further, even the Si-Si vibration is affected, to a lesser extent.

Columns B in Table III show the effect of strained silicon slabs ($k_{Si} \rightarrow 0.9k_{Si}$) on the three principal peaks. This simulates the case of an epitaxial Si_nGe_m structure grown on a Ge substrate and hence the Ge layers are assumed to be unstrained. The shifts (decrease in $\Delta\omega$) of the Ge-Si peaks are larger than those obtained in strained Ge grown on Si substrates (column A). Also, the Ge-Ge peaks are somewhat influenced by the strain in the Si slabs.

These results show that if one set of layers is strained while the others are not (e.g., column A: Ge layers are strained while Si layers are not) it does not necessarily follow that the shift in, say, the Ge-Ge peak unambiguously leads to an estimate of the strain in the Ge slabs. The frequency shifts due to strain depend on the local environment (i.e., values of m,n) in which the vibrating unit is embedded. Our studies on the effect of interface smudging, to be discussed in the next section, will further emphasize this and hence it seems that extreme caution is necessary in interpreting Raman spectra of commensurate or incommensurate alloy structures, random structures or structures grown on alloy buffers, or in comparing them with the spectra of superlattices. The number of Ge—Ge, Si—Ge, or Si—Si bonds and the local strain environment found in a local cluster in a random alloy is unknown and hence conclusions about strain, confinement, etc. are open to a high degree of error.

The effect of strain on a Ge_6Si_6 system where the interface layers are smudged due to admixture of the other component (15% and 30%) is also shown in Table III. The effects are particularly drastic in the B columns since in this case the smudging and the strain work in the same direction. We discuss interface smudging in the following section.

V. THE EFFECT OF INTERFACE SMUDGING

In the preceding sections we studied the behavior of optical-phonon spectra for ideal Ge_mSi_n superlattices as a function of m, n, and strain. We assumed that the interfaces are ideal in that we pass from a pure Ge atomic layer to a pure Si atomic layer or vice versa at an interface. Under practical growth conditions the two interface layers are likely to become modified due to kinetic and other processes associated with epitaxial growth. Hence, to simulate experimental conditions it becomes necessary to incorporate interface-"smudging" effects. The linear-chain model really treats vibrations of whole planes of atoms. Hence, instead of the ideal atomic masses, force constants, and polarizabilities, we need the "smudged" values which correspond to average values over whole planes perpendicular to the direction z defined by the linear-chain model. In practice the averages extend only over a characteristic length in the x-y plane corresponding to the damping distance of the interactions in the planes. At present no microscopic information of this sort is available and hence we resort to simple models. To begin with let us assume that smudging affects

only one atomic layer on both sides of an interface. That is, if we consider a Ge/Si interface, the Ge atom will be replaced by an atom of mass m_h, [Eq. (5.1a)] while Si will be replaced by an atom of mass m_l, [Eq. (5.1b)] where h and l designate the "heavy" and "light" atomic layers of the interface. In the following we will use m_h and m_l to indicate the mixed layers.

Hence we write

$$(\mathrm{Ge}_m\mathrm{Si}_n)_p \rightarrow (m_h\mathrm{Ge}_{m-2}m_h m_l\mathrm{Si}_{n-2}m_l)_p$$

where we now have $m_h m_l$ and $m_l m_h$ interfaces instead of Ge/Si and Si/Ge interfaces, respectively. The masses m_h and m_l are taken to be

$$m_h=(1-x)m_{\mathrm{Ge}}+xm_{\mathrm{Si}}\ , \tag{5.1a}$$

$$m_l=xm_{\mathrm{Ge}}+(1-x)m_{\mathrm{Si}}\ , \tag{5.1b}$$

with $x \leq 0.5$.

The value of the intermixing or smudging parameter x will depend on the growth conditions and could vary from interface to interface. However, we assume that reproducible atomic-layer epitaxy is used for preparing the $\mathrm{Ge}_m\mathrm{Si}_n$ superlattices. Hence, x may take values within a narrow range near some average value x. In fact, we will attempt to show that Raman data allow us to make an estimate of x.

To study the effect of interface smudging on the Raman spectra we examine in detail a specific model system, viz., $(\mathrm{Ge}_6\mathrm{Si}_6)_{24}$ smudged to become $(m_h\mathrm{Ge}_4 m_h m_l\mathrm{Si}_4 m_l)_{24}$ as a function of the fraction of intermixing x which determines the mass m_h and m_l. We have also linearly intermixed the force constants, and polarizabilities of the smudged layers, just as for the masses. In these calculations we assume as usual 500 atomic layers of silicon substrate (or germanium substrate as the case may be) and 37 atomic layers (50 Å) of Si cap (or Ge cap) although their presence does not appreciably affect the positions of the optical-phonon peaks studied here.

In Fig. 4 we show how the spectrum of the ideal $(\mathrm{Ge}_6\mathrm{Si}_6)_{24}$ structure, $x=0$, evolves as x is increased. The calculated spectra look very like the actual spectra of experimental samples, with a three-mode behavior.[15] The spectrum with 10% intermixing ($x=0.1$) is very similar to the typical experimental spectrum with a mode near 417 cm^{-1} generally described loosely as a Ge-Si mode. Figure 5 shows the vibration amplitudes for the case $x=0.15$, with some of the interface layers marked by dashed vertical lines. The 405-cm^{-1} mode clearly involves excitation of the "Ge-Si" interface layers.

Table IV shows the evolution of the three peaks as a function of x, the fraction of intermixing. These calculations do not include strain. Thus a 15% intermixing would give rise to an *unstrained* Ge-Si-like mode near 405 cm^{-1}. The Ge-Ge-like peak is raised to 301 cm^{-1}, i.e., it is higher than the bulk value. This *increase* is due to the admixture of lighter Si atoms and not due to strain. Similarly, the so-called "Ge-Si" mode is more properly identified as a silicon slab mode (partially antisymmetric mode) weighed down by an admixture of heavier Ge atoms. This 405-cm^{-1} mode would move upwards, typically to 408 cm^{-1} (see Table III) if lattice strain is included and could constitute the so-called "Ge-Si"-like mode of experimental spectra. In Fig. 5 we show the vibrational amplitudes for the three modes in a system with 15% smudging. It is clear that the "Ge-Si"-like mode is really a Si-Si-Si-Si mode bounded by smudged Si layers, m_l (Si layers with Ge admixture), at the two ends forming the interface layers.

The implication of the results of Table IV is that Ge-Ge-like modes appearing at a higher frequency than that of the bulk Ge-Ge mode (viz., 300 cm^{-1}) do not necessarily imply strain. While partially confined unstrained unsmudged Ge-Ge modes fall below 300 cm^{-1} (see Table II), the corresponding peaks in nonideal superlattices or alloys will tend to lie above the bulk value due to the admixture of lighter Si atoms into the smudged interface planes. Similarly, the so-called "Ge-Si"-like peak could lie above, below, or near the extended Ge-Si mode at 417 cm^{-1} typical of the $m=1$, $n=1$ zinc-blende structure $(\mathrm{GeSi})_p$. In fact, it may be misleading to relate the experimental peak near 390–425 cm^{-1} to the Ge-Si zinc-blende peak, as will be seen later, in our discussion of experimental spectra. Similar caution is needed in interpreting the position of the Si-Si peak in terms of confinement and strain alone. Confinement lowers the Si-Si peak from the bulk value of 520 cm^{-1} (see Table II). But so does admixture of germanium, as seen from Table IV. If the Si layers are lattice matched to a Ge substrate the strain also lowers the Si-Si peaks (see Table III) and hence the interpretation of alloy spectra as well as superlattice spectra requires a careful treatment of local m,n in

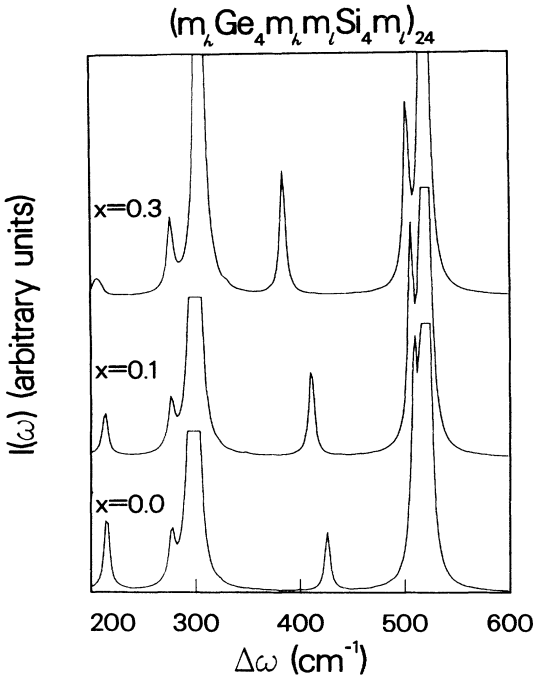

FIG. 4. Evolution of the spectrum of $(\mathrm{Ge}_6\mathrm{Si}_6)_{24}$ as interface smudging is increased from $x=0$ (no smudging) to $x=0.3$ where the Si interface layer has 30 at. % Ge and the Ge interface layer has 30 at. % Si atoms. The strong peak at 520 cm^{-1} arises from the substrate and cap Si layers.

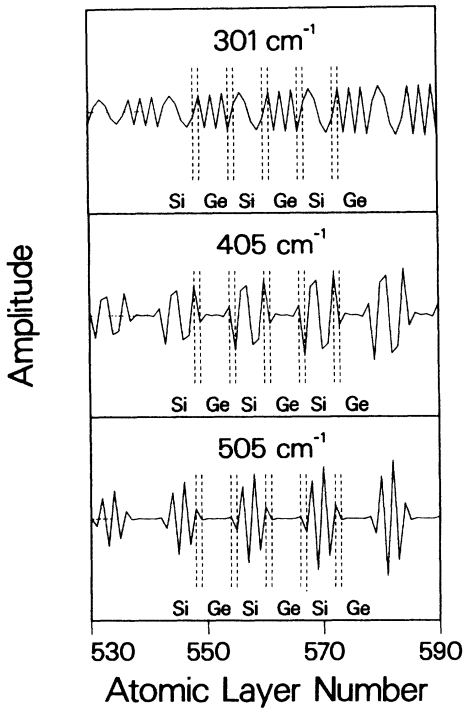

FIG. 5. The vibration amplitudes of the three optical-phonon modes of $(Ge_6Si_6)_{24}$ with 15% interface smudging. Note that the mode at 405 cm^{-1} involves the interface layers (shown as dashed vertical lines) and its position depends on interface smudging. The Ge-Ge mode at 298 cm^{-1} in the ideal unsmudged Ge_6Si_6 has moved up to 301 cm^{-1} in this unstrained smudged system. The Si-Si peak, ideally at 509 cm^{-1}, has moved down to 505 cm^{-1}.

the relevant Ge_mSi_n structure, its strain, confinement, and "interface" smudging.

In this discussion of interface smudging we have treated the interface of Si on Ge in essentially the same way ("symmetric model") as the interface of Ge grown on Si. However, since the growth kinetics of Si deposition on Ge is different from that of Ge deposition on Si, the interfaces on the two sides need not be similar ("asymmetric model"). As examples of the symmetric and asymmetric models we consider $(m_hGe_4m_hm_lSi_4m_l)_{24}$ and $(m_hGe_4GeSiSi_4m_l)_{24}$ where the latter (asymmetric case) assumes, for instance, that Si growth on Ge leads to a perfect interface while Ge growth on Si leads to a smudged interface. This is, of course, an extreme case and should lead to the largest effects of symmetric versus asymmetric modeling. Calculations for the case $x=0.1$, for example, show that the "Ge-Si"-like mode shifts from 411 cm^{-1} in the symmetric case to 418 cm^{-1} in the asymmetric case. Also, the intensity of the mode decreases. Both these changes are consistent with simple ideas of decrease of confinement, decrease of mass of the Si-like vibrating units, and the decrease in the number of Ge-Si-type bonds. Of the other peaks, viz., Ge-Ge-like and Si-Si-like peaks, the latter is more sensitive and shifts upwards by about 1 cm^{-1}. The shift in the "Ge-Si"-like peak of about 7 cm^{-1} (or less) should be detectable in careful modeling of good experimental data but the asymmetric treatment introduces extra parameters into the simulation. In the present calculation we have used the simple symmetric model noting that the experimental "Ge-Si"-like peaks are fairly broad (we used a broadening parameter $\Gamma=5$ cm^{-1} in modeling the experimental spectra, see Sec. VI).

The simple two-atomic-layer interface-smudging model $Ge_mSi_n \rightarrow m_hGe_{m-2}m_hm_lSi_{n-2}m_l$ is not necessarily a universally applicable scheme since each sample must be studied within a "sample"-specific scheme. For systems with very small values of m,n, e.g., Ge_3Si_3, etc., a whole slab (i.e., three atomic layers in all) may get smudged and calculations have to be carried out for each case. In the next section we give examples of the analysis of experimental spectra using the ideas and results presented here.

TABLE IV. Effect of interface smudging on the main Raman peaks of the system (Si substrate)+$(Ge_6Si_6)_{24}$+(Si cap). The Ge_6Si_6 system becomes, on smudging, $(m_hGe_4m_hm_lSi_4m_l)_p$ where the masses m_h and m_l are controlled by the smudging parameter x, Eq. (5.1), which is the fractional intermixing. Peak positions are given in cm^{-1}.

x	$\Delta\omega$(Ge-Ge)	$\Delta\omega$(Ge-Si)	$\Delta\omega$(Si-Si)
0.0	294	427	509
0.10	300	411	506
0.15	301	405	505
0.20	302	399	504
0.30	307	381	501
0.50	317	375	501

VI. ANALYSIS OF EXPERIMENTAL SPECTRA

Several laboratories (including ours) have studied Ge_mSi_n ultrathin superlattices grown on silicon substrates, germanium substrates, Ge/Si-alloy substrates, using different growth temperatures. X-ray diffraction data and cross-sectional transmission electron microscopy (XTEM) of such Ge_mSi_n superlattices show overall good epitaxial growth for suitably low values of m or n, depending on the substrate and the growth conditions. However, Raman spectra of these ultrathin superlattices show a characteristic three-mode behavior. Other weaker spectral features, some of which correspond to folded modes and other expected features of these superlattices, are also observed. The almost ubiquitous appearance of the three-mode behavior, with a "Ge-Si" peak around 390–425 cm^{-1} shows that there is considerable intermixing and interface smudging in most experimental samples. Also, a "nominal" Ge_mSi_n structure, where m,n are the target values, may have a distribution of other values m',n' which may differ considerably from the target values, due to various kinetic processes and uncertainties associated with MBE growth.

In analyzing an experimental spectrum we proceed by noting that, say, if the substrate is silicon, then (a) positions and intensities of the high-energy siliconlike peaks will give an *indication* of the actual values of n in the

sample, (b) the position of a given peak is affected by at least three factors, viz., quasiconfinement, strain, and layer smudging, (c) the so-called Ge-Ge peak (near 300 cm^{-1}), or the "Ge-Si" peak (near 415 cm^{-1}), being dependent on many factors, does not give clear indications of the actual values of m,n in the sample, and (d) the observation of superlattice peaks is a better indicator of the dominant values of m and n in the sample. Our approach is to compare the experimental spectrum with the calculated spectra of the target structure and structures close to it with and without strain and interface smudging. The movement of the peaks under annealing is also a useful guide to the existence of strain in various slabs of the superlattice. The experimental spectrum is then constructed as a weighted sum of theoretical spectra arising from a few dominant structures. In other words, we assume that the superlattice is a concatenation of several structures, arranged in series, and in some random order determined by the complexities of the growth kinetics. In practice, if the growth conditions are optimal one of the structures will predominate together with perhaps some other minority structure. Hence fitting to two structures may be adequate. In order to simplify the modeling of such a system we have assumed that the total spectrum can be considered to be the weighted sum of the spectra of the two structures calculated independently.

In fitting the experimental spectra to the calculations the parameters of the majority structure (defined by the crystal growth parameters) usually needed no adjustment, as in the case of the Ge_2Si_6 structure to be discussed presently. In the case of the minority structure adjustable parameters arise in modeling the smudged layers (e.g., the intermixing fraction x and the degree of strain). The majority structure itself may require smudged interfaces. Hence assuming symmetric smudging of the interfaces we have two adjustable parameters per structure to get the peak positions properly aligned. The intensities are fitted by modifying the bulk bond polarizabilities of Si and Ge. The type of agreement between experiment and theory obtained here needed only a modest effort but any further improvements seem to be very difficult. However, there is no clear guarantee that the chosen parameters and structures are unique, although our experience is that the freedom of choice is limited, not only by the experimental spectrum, but also by the need for consistency with other characterization data.

A. Samples grown on Si(001) and Ge(001) substrates

Superlattices of the type Ge_2Si_2, Ge_2Si_4, Ge_2Si_6, Ge_4Si_4, and Ge_4Si_8 were grown on silicon (001) substrates, usually at a growth temperature of 400±25 °C, and capped with a 50–100 Å Si epitaxial layer. The Ge and Si growth rates were set at 0.4 Å/sec for all layers. For epitaxial growth on Ge(001) substrates, a growth temperature of 350 °C was used. Structures corresponding to Si_2Ge_6, Si_2Ge_{12}, Si_2Ge_8, and Si_4Ge_8 were grown (see Ref. 16). The Raman spectra were measured at room temperature in a helium atmosphere, in a pseudobackscattering configuration.[8] Laser light at 458 or 468 nm was used to excite the spectra which were analyzed with a Spex Industries No. 14018 double monochromator.

In all the superlattices grown on Si(001) substrates, typical Ge-Ge-like peaks were found to lie between 297 and 306 cm^{-1}, while the "Ge-Si"-like peak varied from 412–418 cm^{-1}. The position of the Si-Si-like peak was usually more informative and corresponded to the value predicted from Table I, but usually additional peaks, which implied the existence of strain or other values of n, were observed. Also, in many samples enhanced intensity features corresponding to the folded acoustic modes could be identified. The superlattices grown on Ge(001) substrates showed Ge-Ge-like peaks in the range 296–300 cm^{-1} while the "Ge-Si"-like peak position varied from 389.7 to 393.6 cm^{-1}. We confine our detailed discussion to two selected samples, both of which were deemed to be "good" crystals if judged in terms of double-crystal x-ray diffraction (DCXD) data, by XTEM, and other characterization criteria.[6] To be more specific, the two samples showed pseudomorphic growth, with continuous layers. The superlattice grown on (001) Si showed planar growth near the substrate-superlattice interface, while some waviness was apparent in layers away from the interface, probably indicating that two-dimensional growth is not easily maintained for superlattice growth on Si at 400 °C. In the case of the superlattice grown on the (001) Ge substrate, planar growth was generally observed despite some bending of the atomic layers near the substrate-superlattice interface (for XTEM photographs, etc., see Ref. 16). It should be borne in mind that if the crystal deviates strongly from planar growth the linear-chain model should not provide a good description of the system.

1. $(Ge_2Si_6)_{48}$ grown on silicon (001)

This nominal $(Ge_2Si_6)_{48}$ sample was grown by MBE and capped with a 50-Å silicon layer. The experimental Raman spectrum is shown in the bottom panel of Fig. 6. The high-frequency spectrum ($\omega \geq 100$ cm^{-1}) shows strong features near 199, 295, 415, and at 512.5 cm^{-1} (see Fig. 7 for the last peak). The strong peak at 520.1 cm^{-1} originates from the substrate. Broad weaker features are seen at 100–140, 230–270, 330–350, and 425–440 cm^{-1}.

The spectrum calculated for the *unstrained* structure (Si substrate)+$(Ge_2Si_6)_{24}$+(Si cap), with free-surface-boundary conditions ($\sigma=0$) gives Raman peaks at 103, 201, 294, 427, and 509 cm^{-1} (see Table II, entry under Ge_2Si_6). These peak positions were not affected by changing the surface boundary conditions. Note that the calculations are done for $p=24$ superlattice periods, while the experimental spectrum has $p=48$. This has the effect of giving a somewhat lower intensity to the calculated folded mode intensities while the peak positions remain unchanged. Also, we have used 900 layers to simulate the substrate which is several μm thick and optically penetrated up to several thousand angstroms. The use of a small number of substrate atoms has the effect of giving a broader distribution about the 520-cm^{-1} bulk peak, and also giving a poor representation of the intensity relationship between the calculated Si-Si superlattice

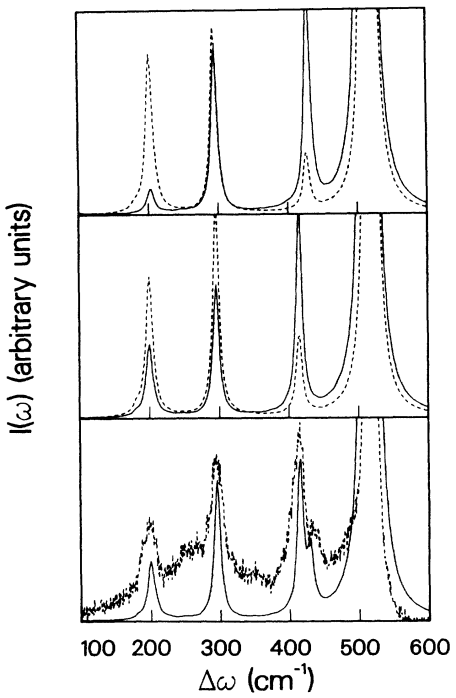

FIG. 6. Reconstruction of the experimental Raman spectrum of sample 1, nominally Ge_2Si_6 on Si(001) (bottom panel), from theoretical spectra. Top panel: dashed line—theoretical spectrum of $(Ge_2Si_6)_{24}$ on 900 atomic layers of Si substrate and capped with 27 atomic layers of Si; solid line—same spectrum with the Raman polarizability a^{xy} of Si in the superlattice enhanced, and Si-Si force constants increased by 1.4%. Middle panel: dashed line—theoretical spectrum of (Si substrate)+$(Ge_2Si_6)_{24}$+(Si cap) with 7.5 at.% intermixing at the interfaces and increase of k_{Si} by 3%; solid line—same with a^{xy} of Si layers of superlattice enhanced. Bottom panel: dashed line—experimental spectrum; solid line—theoretical model spectrum obtained by adding 75% and 25% of solid curves of middle panel and top panel.

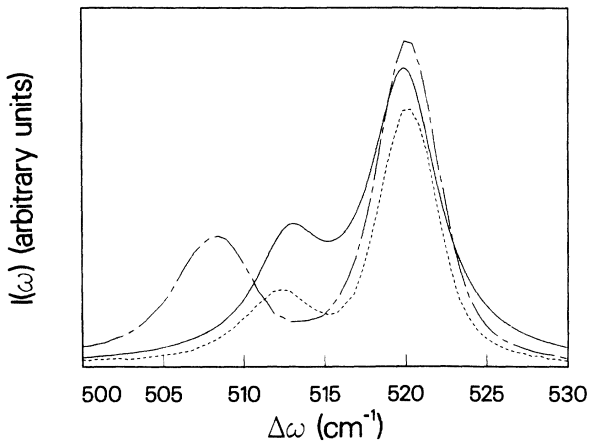

FIG. 7. Annealing study of high-frequency Si peaks for Ge_2Si_6 sample studied in Fig. 6. The solid line is the best-fit theoretical Raman spectrum of Fig. 6 with some modifications (see text). The other curves are the experimental Raman spectra taken from the unannealed (dashed line) and annealed (chained line) sample. After annealing for 15 min the superlattice Si peak drops from 512.5 to 508.2 cm^{-1}. The relative intensities for the three curves are arbitrary.

and substrate peaks. These limitations should be borne in mind in comparing the relative intensities of experimental and theoretical spectra although, of course, the peak *positions* are not affected.

The experimental spectrum contains perhaps only a shoulder at 509 cm^{-1}, while the well-formed experimental Si-Si peak (see Fig. 7) is at 512.5 cm^{-1}. From Table II we might conclude that the structure probably contains Si_7 and Si_8 slabs as well as the Si_6 slabs targeted by the growth conditions. Thus we may expect to see spectral features corresponding to $Ge_{2\pm1}Si_{6\pm1}$ or $Ge_{2\pm1}Si_{6\pm2}$ in this spectrum. Alternatively, if the nominally strain-free Si slabs had a small amount of strain ($\approx 1\%$ change in k_{Si}) the calculated frequency for ideal Ge_2Si_6 of 509 cm^{-1} would shift to the observed value of 512.5 cm^{-1}. Comparison of the observed features of the experimental spectrum (bottom panel of Fig. 6) with the predictions of Table II for unstrained systems, as modified by Tables III and IV for strain and smudging, enables us to explain most of the features in the experimental spectrum. For simplicity we will consider the main spectral features. The strong well-formed low-frequency peak at 199 cm^{-1} in the experimental spectrum is consistent with the theoretically predicted superlattice peak (a "folded mode") at 201 cm^{-1} from $(Ge_2Si_6)_{24}$. It is also found that the 199-cm^{-1} peak is strongly affected by annealing, which would be expected for such a folded mode. A closely related structure, e.g., Ge_1Si_7, has a peak at 189 cm^{-1}. Hence, admixture of lighter Si atoms due to smudging of Ge_1Si_7 could also give rise to a frequency near 200 cm^{-1}. On the other hand, the structures $(Ge_2Si_8)_p$ and $(Ge_2Si_7)_p$ have peaks at 174 and 238 cm^{-1}, respectively. The absence of such features in the experimental spectrum enables us to conclude that Ge_2Si_7- and Ge_2Si_8-type structures are not present in the sample. Similar considerations enable us to eliminate Ge_3Si_7- and Ge_3Si_5-type structures. On the whole, we conclude that the experimental sample contains the target structure Ge_2Si_6, as well as structures derived from Ge_2Si_6 by interface smudging, together with a possibility of some Ge_1Si_7 or Si_8 regions.

Now we consider the Ge-Ge-like peak observed at 295 cm^{-1}. The unstrained unsmudged $(Ge_2Si_6)_p$ and $(Ge_1Si_7)_p$ structures should have peaks (see Table II) at 294 and 189 cm^{-1}, respectively. Thus the 295-cm^{-1} peak is essentially entirely due to the $(Ge_2Si_6)_p$ species, with a small upward shift of ≈ 1 cm^{-1}. This upward shift may be entirely due to strain effects, or due to interface-smudging effects (admixture of the lighter Si raises the Ge-Ge frequency). The fact that the superlattice peak ideally at 201 cm^{-1} is observed at the *lower*-frequency 199 cm^{-1} strongly suggests interface smudging rather than strain. Table III shows that the Ge_2Si_6 structure is less sensitive to strain than the other structures given there. If the observed 1-cm^{-1} shift is entirely due to strain, it still implies that the Ge layers have a strain of less than 5% of the expected strain for Ge epitaxially grown on Si. These considerations suggest that the strain

in the Ge layers has become negligible due to interface-smudging effects. Such a relaxation would be most effective in Ge_2Si_n systems since both Ge layers would become smudged layers. The presence of a strong "Ge-Si"-like peak at 415 cm^{-1} also suggests that interface smudging is present. A calculation involving 7.5% intermixing (i.e., $x=0.075$) of the interface layers gives a spectrum with peaks at 199, 297, 415, and 507 cm^{-1}, in good agreement with the experimental peaks at 199, 295, and 415 cm^{-1}, while the calculated 507-cm^{-1} peak is not in agreement with the 512.5-cm^{-1} peak of the experimental spectrum.

A possible explanation of the origin of the 512.5-cm^{-1} peak is provided by the results of annealing studies. In Fig. 7 we show how the Si-Si peak at 512.5 cm^{-1} shifts when the superlattice is annealed. The 15-min anneal brings the peak down to 508.2 cm^{-1}, i.e., essentially to the calculated value of 507–509 cm^{-1}. We may interpret the annealing process as contributing to the *removal* of some residual strain in the (nominally unstrained) Si layers. The *assumption of the existence of a small amount of strain in the silicon layers,* sufficient to *increase* the Si-Si force constant by 3%, enables us to understand all the features of the Raman spectrum as well as the behavior of the system under annealing. The theoretical curve shown in Fig. 7 will be described later in this paper, while a more detailed analysis of the annealing studies will be reported elsewhere.

We may now attempt to "synthesize" the observed spectrum as being made up of contributions from unsmudged Ge_2Si_6 layers and from those with 7.5% intermixed interface layers. Such a theoretical "simulation" spectrum, where the amount of ideal interfaces is taken to be 25%, is shown in Fig. 6 (bottom panel). This simulation spectrum is arrived at in the following way. The calculated spectrum of the ideal unstrained Ge_2Si_6 structure, using the standard values of the Raman polarizabilities (Table I), is shown as a dashed curve. A broadening parameter $\Gamma=5$ cm^{-1} is used throughout Fig. 6. The intensity of the Si-Si mode at 427 cm^{-1} in the calculated spectrum is quite weak compared to that in the Ge-Ge mode. Hence we increased the value of a^{xy} for Si from 1.59 to 3.5, while retaining the standard value of a^{xy} for Ge at 4.07. The enhanced spectrum is shown as a solid line in the top panel of Fig. 6. The Si-Si force constants in this "enhanced" spectrum have been increased by 1.4% to move the 509-cm^{-1} peak to 512.5 cm^{-1}, as justified by annealing data. This also moves the 427-cm^{-1} peak to 429.5 cm^{-1} but has little effect on the other peak positions. The dashed curve in the middle panel of Fig. 6 is the calculated spectrum of Ge_2Si_6 smudged ($x=0.075$) to form the structure $(m_h)_2(m_lSi_4m_l)$ where m_h indicates a Ge-like layer with 7.5 at. % admixture of Si and m_l is a Si-like layer with 7.5 at. % admixture of Ge. The solid line in the middle panel shows the same case with a^{xy} for Si enhanced to 3.5. In both these curves the Si-Si force constants k_{Si} have been enhanced by 3%, while the force constants of the smudged m_l and m_h layers have been reduced from the bulk values (Table I) by 2% and 4%, respectively.

The theoretical simulation spectrum given as the solid line in the bottom panel is obtained from the weighted sum of the enhanced slightly strained Ge_2Si_6 spectrum (solid line, top panel) using a weight of 0.25, with the spectrum of the enhanced slightly strained 7.5 at. % smudged system (solid line, middle panel) taken with a weight of 0.75. This reconstruction of the experimental spectrum is in good ageement with the results for the average composition, and the total thickness of the structures obtained from XTEM and double-crystal x-ray diffraction data.[16]

In this reconstruction we have had to modify the bond-polarizability factors in order to get the correct relative intensities of the major peaks. This was done in a limited manner without attempting a detailed optimization. Further, the 199-cm^{-1} peak, being essentially a folded superlattice peak, would in any case come out to be weak due to our use of a $(Ge_2Si_6)_{24}$ structure instead of the experimental $(Ge_2Si_6)_{48}$ structure. Similarly, the width of the substrate peak near 520 cm^{-1} is broader than the experimental peak due to the use of a small number of layers for the substrate. Finally, since bond polarizabilities are related microscopically to the band structure of the material in question, it is probably not surprising that the a^{xy} factors needed for a Ge_mSi_n structure are different from those obtained in bulk materials.

The theoretical curve given in Fig. 7 is essentially the same as the theoretical reconstruction shown in the bottom panel of Fig. 6, with some significant differences. Since in Fig. 7 we are comparing the 520-cm^{-1} substrate peak with the Si-Si superlattice peak, we have attempted to get the relative intensities "visually" correct in the following way. Instead of using 900 layers of substrate with 24 periods of the superlattice and $\Gamma=5$ cm^{-1}, as was done for Fig. 6, we have used 1150 substrate atomic layers with 18 periods of the superlattice and $\Gamma=2.5$ cm^{-1} to construct the theoretical spectrum of Fig. 7. These changes reduce the calculated width of the 520-cm^{-1} peak of the substrate and also increase its intensity. In effect these changes are an attempt to get a reasonable representation of the substrate within the limitations of our computer. We stress that the above leads to minimial effects on the peak *positions.* The synthesized spectrum is, as before, composed of 25% of a Ge_2Si_6 structure and 75% of the smudged structure.

The surprising conclusion regarding the nominal $(Ge_2Si_6)_p$ structure studied here is that the Ge layers, having become smudged, carry little strain, while the Si layers have acquired a small amount of strain sufficient to drive the unstrained Si-Si peak near 509 cm^{-1} to the observed 512.5-cm^{-1} peak. Further annealing studies are necesary to determine if the Ge peaks would relax in a manner consistent with Ge layers being relatively free of strain, or whether a different interpretation of the experimental spectrum would become necessary.

It should be noted that XTEM data show the present sample to be a pseudomorphic structure. This is not inconsistent with the present conclusion that the Ge_2 layers [which have become m_h layers] carry little strain. The usual estimate of strain in the Ge layers is based on the mismatch between the equilibrium bond lengths of *bulk* Ge and Si. The equilibrium bond lengths relevant to just

two interface atomic layers of Ge need to be determined, possibly by *ab initio* density functional calculations, before realistic estimates of strain in the atomic-layer structures can be obtained.

2. $(Si_4Ge_8)_{24}$ grown on a Ge(001) substrate

The dashed curves in the bottom panels of Figs. 8 and 9 show the experimental spectrum of a nominal $(Si_4Ge_8)_{24}$ structure grown on a Ge(001) substrate and capped with approximately 20 layers of Ge. The spectrum shows well-formed peaks at about 96.4, 298, 390, and 472 cm^{-1}. Weaker features are seen near 195, 235, and 418 cm^{-1}.

The theoretical spectrum for the unstrained ideal Si_4Ge_8 structure is shown as a dotted line in the top panel of Fig. 8. The solid curve is obtained by introducing strain alone (no smudging) into the Si layers so that the main Si-Si peak at 500 cm^{-1} drops to 472 cm^{-1}. A similar lowering of the 500-cm^{-1} peak can be achieved by a mixture of strain and smudging, or smudging alone. However, all these approaches lead to the presence of an extra peak located at 300–350 cm^{-1}, depending on the type of strain plus smudging mixture used. Strong smudging of the Ge-interface layers also tends to move the Ge-Ge peak into the >300-cm^{-1} range because silicon admixtured layers are lighter. However, the experimental spectrum presents no evidence for a feature in the 300–350-cm^{-1} region and hence structures based on Si_4Ge_8 cannot be used to explain the presence of the 472-cm^{-1} peak *unless* the intensity of the partially antisymmetric mode ($\approx$300–350 cm^{-1}) could be diminished without at the same time reducing the intensity of the fully antisymmetric mode ($\approx$472–500 cm^{-1}).

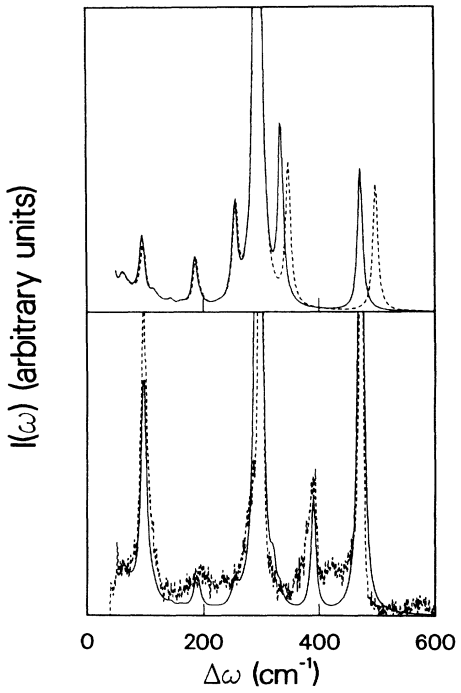

FIG. 8. Reconstruction of the experimental spectrum (bottom panel) of sample 2, nominally Si_4Ge_8 grown on Ge(001). Top panel: dashed line—theoretical spectrum of (Ge substrate)+$(Si_4Ge_8)_{24}$+(Ge cap); solid line—same with the force constant of Si decreased to bring Si-Si peak in line with experimental peak at 472 cm^{-1}. Bottom panel: dashed line—experimental spectrum; solid line—theoretical model spectrum (see Fig. 9 for details).

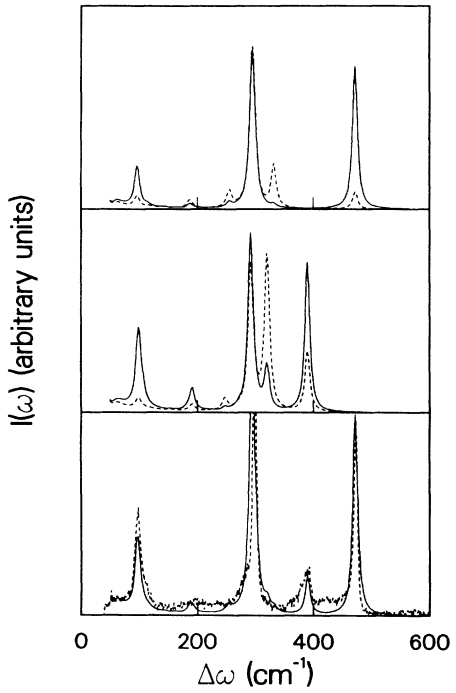

FIG. 9. Top panel: dashed line—Raman spectrum of structure *A*, viz., $(Si_4Ge_6)_{24}$ on Ge substrate with 5 at. % smudging of interfaces and strained Si layers, calculated using bulk bond-polarizability factors a^{xy}; solid line—Raman spectrum with modified a^{xy}. Middle panel: Raman spectrum of structure *B*, viz., $[(m_l)_4 m_h Ge_4 m_h]_{24}$ on Ge substrate, where all the Si atomic layers are intermixed (31 at. %) with Ge, while the heavy layers are 50 at. % Ge. Dashed and solid lines are calculated with bulk and modified a^{xy} values, respectively. Bottom panel: dashed line—experimental spectrum; solid line—theoretical spectrum made up of 80% of (top panel, solid curve) structure *A* and 20% of (middle panel, solid curve) structure *B*.

After a careful study of many possible smudged and strained structures derived from the target structure $(Si_4Ge_8)_p$ we found that the best agreement with the experimental Raman spectrum could be obtained by considering two dominant structures *A* and *B*. The actual physical structure is considered to be made up of 80% of *A* and 20% of *B*. The structure *A* is essentially the target structure $(Si_4Ge_8)_p$ except that the interface layers are smudged due to 5% intermixing, giving the form $(m_l Si_2 m_l m_h Ge_6 m_h)_p$ where the m_l layer contains 95 at. % of Si and 5 at. % of Ge. Similarly the m_h layer contains 95 at. % of Ge and 5 at. % of Si. The m_h layer and Ge layers are assumed unstrained as the system is epitaxial with Ge(001). The assumption that the Ge layers are unstrained seems to be in accordance with the results of annealing studies as well. The Si layers as well as the m_l layers contain about 9% strain in the sense that the Si-Si force constants used were 91% of the bulk value.

The calculated Raman spectrum for this system (structure A), using the bulk bond polarizabilities, is shown in Fig. 9 (dashed line of the top panel). As in the case of the Ge_2Si_6 superlattice discussed previously, we find that the bulk bond polarizabilities do not give a proper description of the observed spectra. The final form adopted involves an enhancement of a^{xy} for the superlattice Si layers from the bulk value of 1.59 to 6.0, while the value of a^{xy} for the smudged silicon (m_l) layers were taken to be 3.5. The polarizability factor for the heavy layers (i.e., m_h layers) had to be lowered to 1.0 (from the usual Ge value of 4.07) and this had the effect of suppressing the intensity of the peak near 320 cm^{-1} to negligible values. The Raman spectrum for the structure A calculated with these modified bond-polarizability factors is shown as a solid line in the top panel of Fig. 9. The second structure, B, contributing 20% to the experimental spectrum is best modeled as $[(m_l)_4(m_h Ge_6 m_h)]_p$. That is, all four Si atomic layers have undergone intermixing to give on average 69 at. % Si and 31 at. % Ge for the light layers. The heavy layers contain 50 at. % Ge and 50 at. % Si. The smudged silicon (m_l) layers are strained to the extent of about 11% in the sense that the force constants used were 89% of the bulk values. The Raman spectrum of the structure B, calculated using the bulk bond-polarizability factors, is shown as a dashed line in the middle panel of Fig. 9. The spectrum calculated with modified values [viz., a^{xy}(light layer)=3.5, a^{xy}(heavy layer)=1.0, and a^{xy}(Ge layer)=4.07, which is the bulk value] is shown as the solid line (middle panel). The bottom panel shows the Raman spectrum of the synthesized structure, made up of 80% of structure A and 20% of structure B. This analysis of the structure of the experimental sample is in good agreement with the overall length and Si/Ge composition determined by other characterization methods (XTEM, DCXD).[16]

VII. CONCLUSIONS

In this paper we have examined the theoretically predicted Raman spectra of $(Ge_m Si_n)_p$-type superlattices using a linear-chain model to calculate the phonons and a bond-polarizability approach to calculate the Raman intensities. The study of the ideal structures enabled us to bring out interesting systematics in the behavior of the Si-Si and Ge-Ge modes under quasiconfinement. The study of the effect of strain and interface smudging showed that these effects have to be included concurrently with confinement in any discussion of experimental spectra. In particular, a discussion based on confinement and strain alone, ignoring the effect of interface smudging, could be seriously in error. That is, smudging shifts the Si-Si- and Ge-Ge-like peaks in addition to bringing out the so-called "Ge-Si"-like peak. The same type of considerations become even more imperative in discussing or comparing alloy spectra since the local environments of the vibrating groups in an alloy are not known. Finally, we have given examples of how an experimental spectrum may be modeled or simulated using spectra calculated for strained and smudged structures derived from the nominal structure $(Ge_m Si_n)_p$. We also showed that annealing studies could be very helpful in resolving some puzzling features and give valuable indications regarding the distribution of strain. The relative magnitudes of the experimental intensities strongly suggest that the bond polarizabilities are modified in these ultrathin $Ge_m Si_n$ superlattices, possibly reflecting changes in band structure. This type of modeling of the experimental Raman spectrum would lead to useful characterization of these $(Ge_m Si_n)_p$-type superlattices, providing some quantitative estimates of interface mixing, strain, and deviation of the actual structure from the target structure.

ACKNOWLEDGMENTS

The authors wish to thank Dr. Karel Kunc (University of Paris) for providing some details regarding first-principles force constants for Ge and Si. Also, the authors are grateful to Dr. José Menéndez (Arizona State University, Tempe, AZ) for details regarding the bond-polarizability model used in the Raman study of Ref. 9. We also thank Dr. Garry P. Schwartz (AT&T Bell Laboratories, Murray Hill, NJ) for helpful information.

[1]J. Bevk, J. P. Mannaerts, L. C. Feldman, B. A. Davidson, and A. Ourmazad, Appl. Phys. Lett. **49**, 286 (1986); E. Kasper, H.-J. Herzog, H. Dämbkes, and G. Abstreiter, in *Layered Structures and Epitaxy*, Vol. 56 of *Materials Research Society Proceedings*, edited by M. Gibson *et al.* (MRS, Pittsburgh, 1986).

[2]D. J. Lockwood, M. W. C. Dharma-wardana, G. C. Aers, and J.-M. Baribeau, Appl. Phys. Lett. **52**, 2040 (1988).

[3]G. C. Aers, M. W. C. Dharma-wardana, G. P. Schwartz, and J. Bevk, Phys. Rev. B **39**, 1092 (1989).

[4]M. A. Maradudin and E. Burstein, Phys. Rev. **164**, 1081 (1967); W. Weber, S. Go, K. C. Rustagi, and H. Bilz, in *Proceedings of the 12th International Conference on the Physics of Semiconductors, Stuttgart (Teubner, Stuttgart, 1974)*, p. 194.

[5]R. J. Bell, Methods Comput. Phys. **15**, 216 (1976).

[6]A. Fleszar and R. Resta, Phys. Rev. B **34**, 7140 (1986).

[7]K. Kunc, in *Electronic Structure, Dynamics and Quantum Strutural Properties of Condensed Matter*, edited by J. Devreese and P. Van Camp (Plenum, New York, 1984), p. 254, Table 5.1

[8]See D. J. Lockwood, M. W. C. Dharma-wardana, J.-M. Baribeau, and D. C. Houghton, Phys. Rev. B **35**, 2243 (1987) for details of the experimental arrangement in the backscattering configuration.

[9]J. Menéndez, A. Pinczuk, J. Bevk, and J. P. Mannaerts, J. Vac. Sci. Technol. B **6**, 1306 (1988).

[10]Bangfen Zhu and K. A. Chao, Phys. Rev. B **31**, 4906 (1987). Details of the reduction of Eq. (2.2) to calculate Raman intensities are given in this paper.

[11]M. Cardona, in *Light Scattering in Solids II*, Vol. 50 of *Topics*

in Applied Physics, edited by M. Cardona and G. Güntherodt (Springer-Verlag, Berlin, 1982), p. 67, Table 2.7.

[12]B. Jusserand, O. Paquet, and A. Regreny, Superlatt. Microstruct. **1**, 61 (1985).

[13]A. Fasolino and E. Molinari, J. Phys. (Paris) Colloq. **48**, C5-569 (1987).

[14]F. Cerdeira, A. Pinczuk, J. C. Bean, B. Batlogg, and B. A. Wilson, Appl. Phys. Lett. **45**, 1138 (1984).

[15]For experimental spectra see Ref. 2, Ref. 9, also E. Kasper, H. Kibbel, H. Jorke, H. Brugger, E. Friess, and G. Abstreiter, Phys. Rev. B **38**, 3599 (1988).

[16]For a discussion of x-ray and XTEM results, see J.-M. Baribeau, D. J. Lockwood, M. W. C. Dharma-wardana, N. L. Rowell, and J. P. McCaffrey, Thin Solid Films (to be published).